Adiabatic Invariants and Diagnostic Studies of Climate

IGOR PISNITCHENKO[1] and MICHAEL KURGANSKY[2]

[1]CPTEC/INPE, Rodovia Presidente Dutra, km 40, 12630-000 Cachoeira Paulista, SP, Brazil
[2]Institute of Atmospheric Physics, Russian Academy of Science, Moscow, Russia

Manuscript received on March, 1996; accepted for publication on October 30, 1996

ABSTRACT

The question of using of adiabatic invariants in climate studies and for verification of General Circulation Model is discussed. Main functionals from these invariants, which are slowly transformed only due to the influences of irreversible processes could be convenient indices of climatic changes. Short review of various diagnostic methods based on the analysis of potential vorticity and potential temperature fields and the functionals from these meteorological parameters in the investigations of weather regimes and climate variability is presented. The example of the use of some of these methods to the analysis of the output data of CPTEC General Circulation Model is given.

Key words: Potential vorticity, non-adiabatic atmospheric systems.

1. INTRODUCTION

Ertel's potential vorticity (PV) (Ertel,1942) and entropy as adiabatic invariants play an important role in modern atmospheric science. Two properties of the PV-field are frequently used in dynamic meteorology: 1) PV is materially conserved for adiabatic motions subject to conservative forces and 2) under some natural balance assumptions, all meteorological fields can be calculated from a known PV-field. But there is a rare use of the concept of potential vorticity in climate studies: some functionals of PV-field may be considered as useful indices of climatic changes. PV-field is slowly transformed due to the influence of irreversible processes (diabatic heating and friction). Thus, the air mass distribution on PV and entropy (or potential temperature - PT) values, which was introduced by Obukhov (Obukhov,1964), significantly changes only on climatic time intervals (one month or longer), thus filtering out synoptic-scale fluctuations.

An isentropic analysis of global atmospheric processes using potential vorticity concept (potential vorticity analysis - PVA), was first carried out by the group of Prof. Brian Hoskins (Haynes & McIntyre,1990; Hoskins *et al.*, 1985) and by the team under the leadership of Prof. Alexander M. Obukhov (Agayan *et al.*,1986; Agayan *et al.*, 1990; Kurganskiy & Tatarskaya, 1987; Kurganskiy, 1993; Obukhov *et al.*, 1988). The FGGE (First Global GARP (Global Atmosphere Research Program) Experiment) data have been used in these studies.

In this article we intend to give a short review of the diagnostic methods, based on the adiabatic invariants concept, which may be used in climate study and in the investigation of the long-term variability of weather regimes such as blocking systems. These diagnostic methods constitute a very convenient instrument for validation of the Global Circulation Models (GCM).

Correspondence to: Igor Pisnitchenko
E-mail: pisnitch@tajyra.cptec.inpe.br

2. APPLYING OF PVA TO STUDIES OF LONG-TERM ATMOSPHERIC PROCESSES

The first step of PVA is to calculate the daily fields of invariants PV and PT. For this aim we used FGGE level IIIa data on the zonal (u) and meridional (v) components of wind velocity and air temperature at 12 isobaric surfaces (1000, 850, 700, 500, 400, 300, 250, 200, 200, 150, 100, 70, 50). We also used geopotential data for interpolating PV on isentropic surfaces.

In our investigations, the PV was taken in normalized form as proposed by Obukhov, (1964):

$$\tilde{\Omega} = (\Omega_z + 2\omega \sin\varphi)\frac{\gamma_a - \gamma}{p}\frac{p^*}{\gamma_a - \gamma^*}, \qquad (1)$$

where Ω_z is the vertical component of the relative vorticity, $2\omega \sin\varphi$ is the Coriolis parameter, γ is the actual vertical temperature gradient, $\gamma_a = g/c_p$ – is the adiabatic temperature gradient and p is the pressure. $p^*(\theta)$, $\gamma^*(\theta)$ are some functions of θ (potential temperature) for normalization, which were considered as the mean climatic values of p, γ on isentropic surfaces. It is convenient to approximate these functions by the following expressions:

$$p^* = A_1 - B_1\, arctan[C_1(\theta - \theta_1)]$$

$$\gamma_a - \gamma^*(\theta) = \frac{p^* g[1 + (C_1(\theta - \theta_1))^2]}{R\theta\, B_1 C_1}$$

where A_1 = 681 mb, B_1 = 434 mb, C_1 = 0.04614 K^{-1}, $\theta_1 = 293$ K, g-gravitational acceleration, R-gas constant of dry air.

Note here, that the normalized PV (1) is a direct result of Ertel's theorem (Ertel,1942) because along with I, any quantity $I \cdot f(\theta)$ will be adiabatic invariant, where $f(\theta)$ is an arbitrary function of the PT. The Ertel vorticity I is useful when it is necessary to distinguish air parcels of tropospheric and stratospheric origin. However, there are also some important drawbacks in using it. First, it displays large variations both with latitude and also with altitude (due to the ρ^{-1} factor) competing in the latter relation with PT. Second, proceeding from Ertel PV, it is impossible to calculate a vorticity charge (very useful characteristic of atmosphere in climatic investigations defined as density weighted integral from vorticity) for the whole atmosphere due to the divergence of this integral. In order to avoid this difficulty, we set $f(\theta) = g^{-1} dp^*(\theta)/d\theta$ (Obukhov, 1964) and define the PV according to the formula (1). In this case, PV is equal to the absolute vorticity reduced to some standard stratification. The PV $\tilde{\Omega}$ mainly varies in the meridional direction, while θ changes mainly in altitude. Therefore, the family of surfaces $\theta = const$ and $\tilde{\Omega} = const$ can be regarded as the coordinate surfaces. This is convenient in many cases, for example, for the interpretation of some climatic functionals such as the air mass distribution on PV, PT surfaces. There is one more advantage for using PV in the form given by (1): the normalization function, selected in an appropriate way, minimizes time-variance of vorticity charge and turn it into quasi-conservative characteristic under the influence of diabatic heating and friction.

For the analysis of the special weather regimes which took place during the FGGE period, the potential vorticity $\tilde{\Omega}$ field was initially calculated on isobaric surface and then interpolated to isentropic surfaces using vertically dependent cubic spline. Fig. 1,b gives one example of such calculation. It shows the potential vorticity distribution on the isentropic surface $\theta = 307$K for NH on 00 GMT, 24 December, 1978. We have used here other isentropic surfaces ($\theta = 307,305,310$ K) because they are entirely located in the troposphere in middle latitudes, close to the 500hPa isobaric surface and nowhere intersect the Earth surface, except at very high mountain peaks. A geopotential field on the 500 hPa isobaric surface for the same date is shown in Fig. 1,a for comparison. Comparing these two maps, we can infer that the blocking formation (vortex pair consisting from a cyclone and an anticyclone) over the North Atlantic in Fig. 1,a (arrow 1) has a conforming structure of similar configuration in Fig. 1,b (arrow 1). This structure shows low potential vorticity (less than $0.5 \cdot 10^{-4}\ s^{-1}$) in the northern part, where the anticyclone is placed, and high potential vorticity (about $3 \cdot 10^{-4}\ s^{-1}$) in the southern part, where the cyclone is located. Considerable meridional ex-

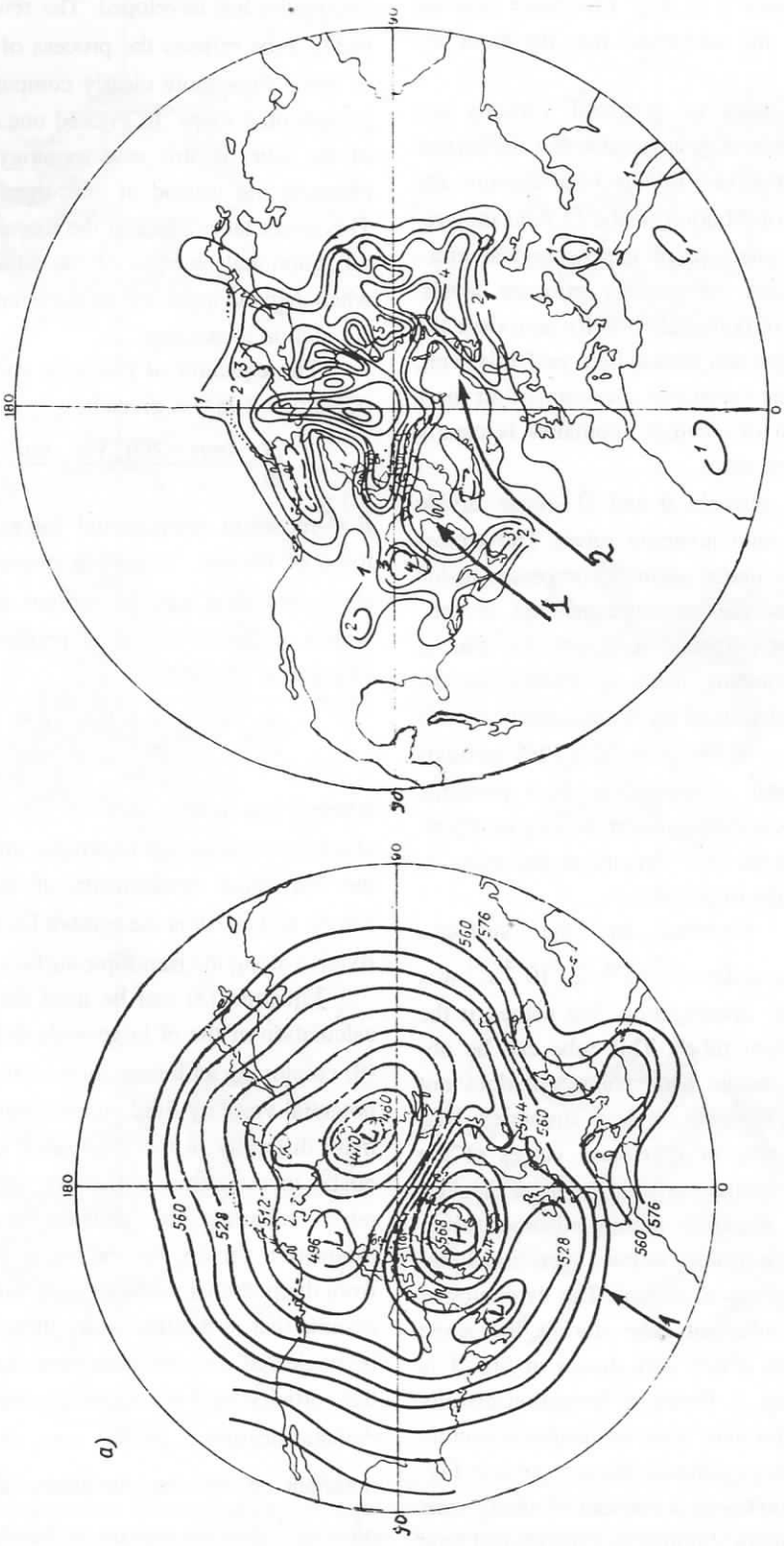

Fig. 1 — Distribution of a) geopotential on the 500 mb surface (contour interval: 16 dm) and b) potential vorticity on the isentropic surface $\theta = 307$ K (contour interval: $1 \cdot 10^{-4}\ s^{-1}$) for the NH on December 24, 1978.

change of air masses occurs during the formation of blocking. Arrow 2 in Fig. 1,b shows how air penetrates from the subtropics into the arctic region.

Isentropic maps of potential vorticity are equivalent to maps of geopotential, but the former are more informative. Taking into account the static stability contribution to the $\tilde{\Omega}$ field they reflect the interconnection of meteorological processes which occur on various pressure levels. Isentropic maps of potential vorticity reproduce the nonzonality of the real atmosphere perfectly well, and the role of the horizontal advection of air mass in the formation of weather anomalies is clearly displayed on these maps.

Coordinate surfaces θ and $\tilde{\Omega}$ *–const* divide the atmosphere onto invariant tubes. The atmospheric air moves under adiabatic processes inside them. The tubes are three-dimensional objects. Their convenient graphical representation can be obtained by projecting them on Earth's surface map. The construction of the appropriately chosen $(\theta,\tilde{\Omega})$-tubes is one of the promising PVA methods in the atmospheric investigation. It is possible, with its help, to get expressive and easily interpretable information on the dynamical processes in the main part of the troposphere.

The tube bounded by the surfaces, $\theta = 305,\ 310\ K$ and $\tilde{\Omega} = 1 \cdot 10^{-4},\ 2 \cdot 10^{-4}\ s^{-1}$ was considered in our investigation. We named it the "reference invariant tube". This tube can be observed over the whole hemisphere and does not disintegrate into separate regional structures. It is situated in the zone of maximum values of the module of the potential vorticity gradient, displaying the smallest thickness among all other tubes. This gives the opportunity to trace meridional displacement with good resolution. The dynamics of such reference invariant tube during the same blocking situation which was shown in Fig. 1 is represented in Fig. 2. Blocking formation distorts the zonal flow and over some hemispheric sectors the flow becomes meridional. We can see it in Fig. 2 a-f. Arrow 1 points to a difluent blocking over North Atlantic; arrow 2 points to a meridional type blocking over Rocky Mountains and Pacific Ocean; arrow 3 points to a sector where cyclonic circulation has developed. The reference invariant $(\theta,\tilde{\Omega})$- tube reflects the process of the breakdown of zonal flow more clearly compared to the usual geopotential maps. In Fig. 2d one can see a break of the tube. In this case topology of the tube is changed and instead of one, there are two tubes. This event takes place at the moment of the greatest individual changes of the adiabatic invariants when diabatic influence on the general atmospheric circulation is maximal.

The equation of potential vorticity evolution (Obukhov, 1964) is given by:

$$\frac{dI}{dt} = \frac{(rot\vec{v} + 2\vec{\Omega}) \cdot \nabla\dot{\theta}}{\rho} + \frac{rot\vec{F} \cdot \nabla\theta}{\rho} \qquad (2)$$

$\vec{F}$ – represent nonpotential forces, including the force of friction. Assuming quasi-geostrophy the above equation can be written in θ-coordinate with a sufficient degree of precision in the form (Agayan *et al.*, 1990;)

$$\frac{d_\theta}{dt}(q^{-1}) = -\frac{\partial\dot{\theta}q^{-1}}{\partial\theta} - \frac{1}{\rho_\theta q^2}\left(\frac{\partial G}{\partial x} - \frac{\partial F}{\partial y}\right), \qquad (3)$$

where $q = \omega_{a\theta} / \rho_\theta$, $\rho_\theta = -g^{-1}\partial p / \partial\theta$, $\omega_{a\theta}$ is the absolute vorticity on isentropic surface, F, G are the horizontal components of the nonpotential forces, and d_θ/dt is the symbol for the material derivative along the isentropic surface.

Equation (3) can be used for the diagnostic calculation of the of large-scale diabatic heat field (θ) employing an information on time series of the potential vorticity field on isentropic surfaces. The main difficulty in the application of (3) for diagnostic investigation is that we cannot simultaneously calculate the diabatic heating and the dissipative factors on the basis of equation (3) from the potential vorticity field only.We therefore assume that in the free atmosphere dissipation can be neglected, i.e., the transformation of the potential vorticity field is completely conditioned by the diabatic heating θ. In this case, shifting from the invariant q to the invariant $\tilde{\Omega} = \rho_\theta^* q$ (with $\rho_\theta^* = -g^{-1}\, dp*/d\theta$, and $p*$ as the standard dependence of pressure with θ) we have:

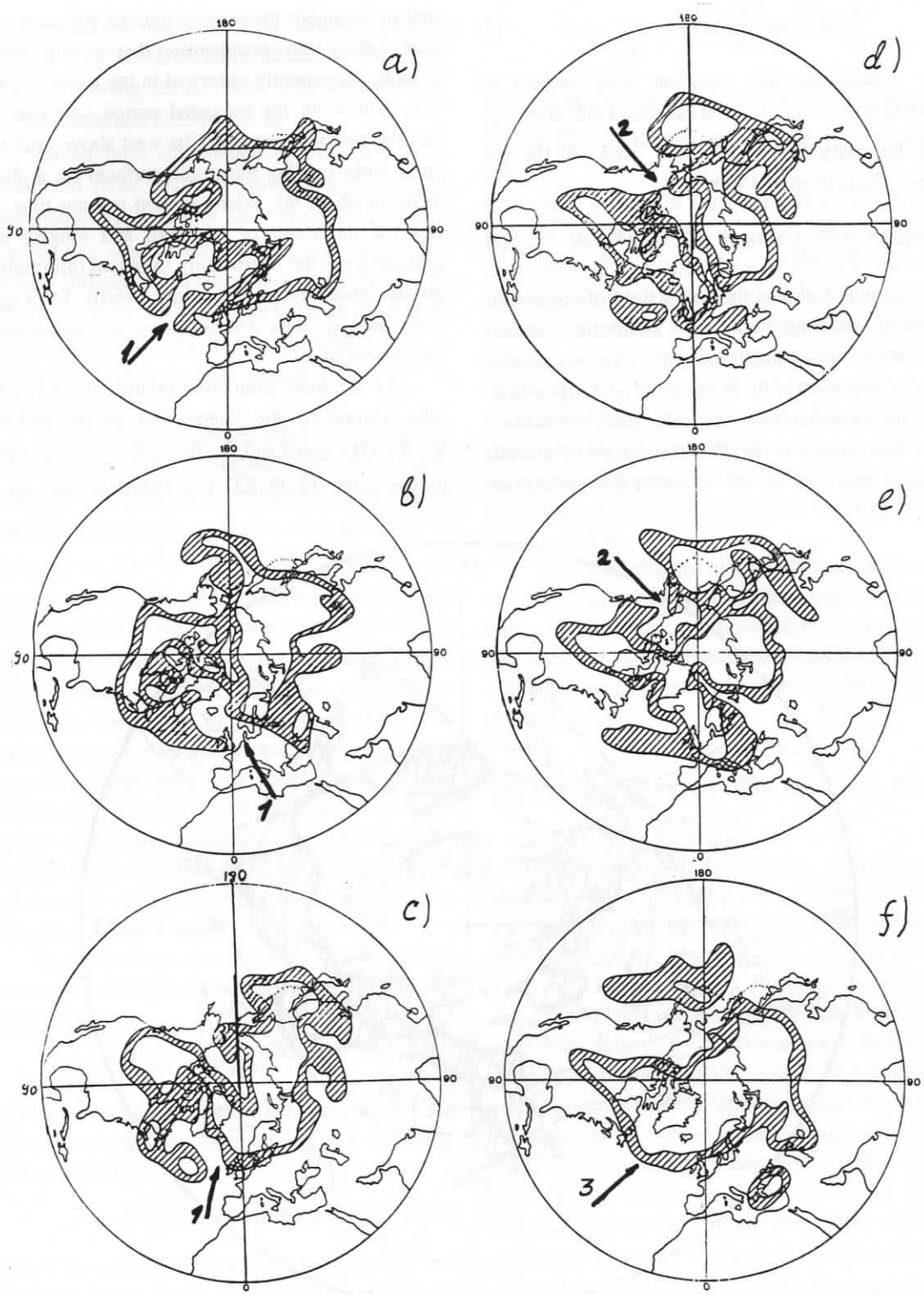

Fig. 2 — Dynamics of "reference invariant tube": a) 24 December 1978, b) 28 Dec, c) 30 Dec, d) 1 January 1979, e) 2 Jan, f) 8 Jan. Arrow 1 points to a difluent blocking over North Atlantic; 2- points to a meridional type blocking over Rocky Mountains and Pacific Ocean; 3 indicate sector where cyclonic circulation is developed. One can see a break of the tube (d), that represent change of topology of the tube and connected with a strong diabatic influence.

$$\frac{d\theta}{dt}\left(\tilde{\Omega}^{-1}\rho_\theta^*\right) \approx -\frac{\partial}{\partial\theta}\left(\tilde{\Omega}^{-1}\rho_\theta^*\dot{\theta}\right) \qquad (4)$$

Integrating this equation with respect to θ from $\theta_0 = const$ to ∞ and assuming that at the upper boundary $\tilde{\Omega}^{-1}\,\theta \to 0$, we arrive at the formula (Agayan *et al.*,1990;):

$$\dot{\theta}_{\theta=\theta_0} = -\frac{\tilde{\Omega}}{dp^*/d\theta}\Big|_{\theta=\theta_0} \int_{\theta_0}^{\infty} \tilde{\Omega}^{-2}\frac{d\theta\tilde{\Omega}}{dt}\frac{dp^*}{d\theta}\,d\theta \qquad (5).$$

Figure 3 shows the mean field of large-scale diabatic heating on the isentropic surface $\theta = 307\ K$, calculated from (5) for the period 12/25/78 to 01/21/79. The regions of positive heating are cross-hatched. The solid lines are isobars. The calculations reveal that the centers of diabatic heating and cooling on the isentropic surface are tied to the major pressure centers on the same surface. Taking into consideration that wavenumber 2 is more prominently observed in the mean circulation pattern for the indicated period, one can see that the heat sources tilt to the west above cyclones (heat sinks on this isentropic surface) on a phase angle of about 90. When applied to long time series (of the order of a month and longer) this method gives the opportunity to obtain information on the mean diabatic heating directly from grid point analysis data without using any parameterization formulae.

An air mass contained in the infinitely thin tube formed by the intersection of the surfaces θ, $\theta + d\theta = const$ and $\tilde{\Omega}$, $\tilde{\Omega} + d\tilde{\Omega} = const$ is equal to $dm = \mu(\theta, \tilde{\Omega})d\theta\, d\tilde{\Omega}$. The function $\mu(\theta, \tilde{\Omega})$ is

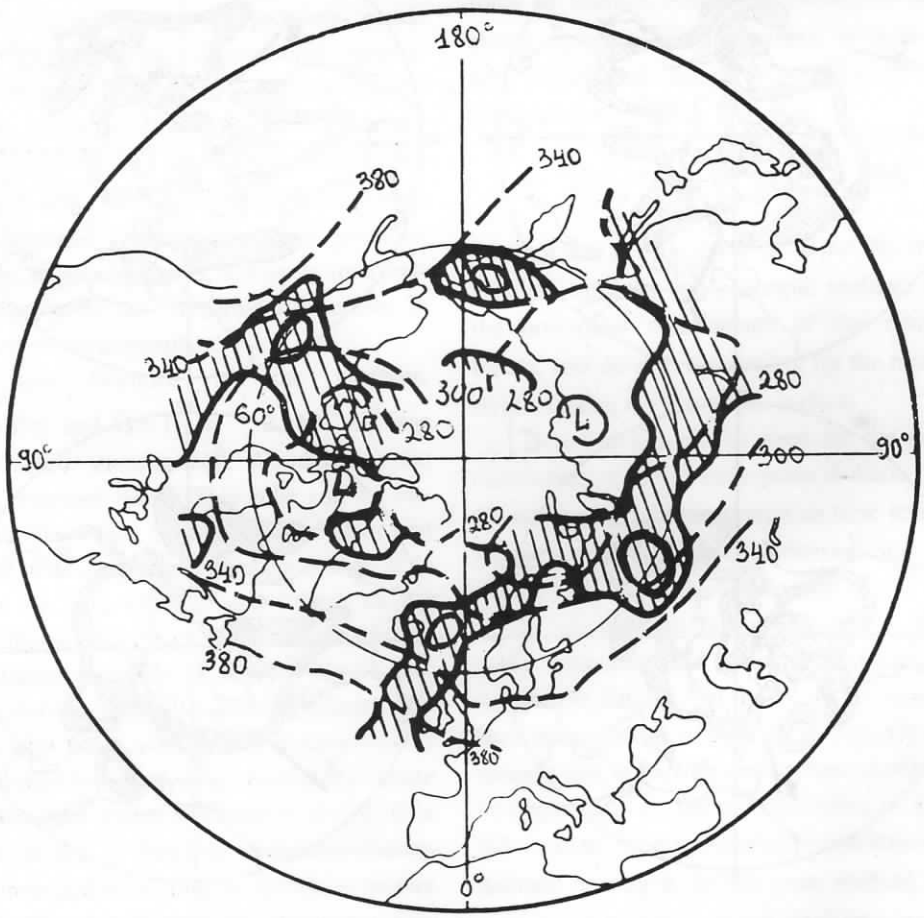

Fig. 3 — The average (for the period from 25 December 1978 to 21 January 1979) field of large-scale heat inflows $\dot{\theta}$ ($K{\cdot}day^{-1}$) (contour interval: 5 K) on the isentropic surface $\theta = 307K$. The regions of positive heat inflows are cross-hatched. The dashed lines are isobars (mb).

also an adiabatic invariant of the atmospheric motion and may be statistically treated as the probability of finding an air mass with the values of adiabatic invariant closed to $\theta, \tilde{\Omega}$.

The air mass distribution $\mu(\theta, \tilde{\Omega})$ have been determined from potential vorticity and potential temperature by summing the values $\Delta \rho_k \cos\varphi_{k,i}$, over the any considered region, where $\Delta \rho_k$ is the pressure difference between the k-th and $(k + 1)$-th isobaric surfaces, between which the air mass with the $\theta \pm \Delta\theta$ and $\tilde{\Omega} \pm \Delta\tilde{\Omega}$ values is located. $\cos\varphi_{k,i}$ is the cosine of geographical latitude for the i – th point on the k surface.

The calculation of the air mass distribution for the entire globe for 1 September 1995 year is given in Fig. 4. The $\mu(\theta, \tilde{\Omega})$ is characterized by the air mass concentration in the region of small values of PV from $-1 \cdot 10^{-4}\, s^{-1}$ to $1 \cdot 10^{-4}\, s^{-1}$, and for PT between 305 – 320 K. Calculation based on the FGGE resulted to the conclusion that the summer distribution of $\mu(\theta, \tilde{\Omega})$ for the Northern Hemisphere is more nonuniform than the winter. It reflects the tendency to the concentration of atmospheric mass in a restricted range of PV values and perhaps there is a consequence of irreversible mixing processes of air mass on isentropic surfaces due to the influence of the friction on the absolute value of PV. In the Southern Hemisphere the seasonal variability of the mass distribution is less pronounced.

Figure 5 shows the time behavior of the first momentum of mass distribution (the atmospheric vortex charge):

$$Z_A = \iint \tilde{\Omega}\mu\,(\theta, \tilde{\Omega}) d\theta\, d\tilde{\Omega} \tag{6}$$

and the informational entropy of mass distribution defined according to Shannon and von Neumann (Katz,1967) is

$$H = -K \cdot \iint \mu(\theta, \tilde{\Omega}) \ln \mu(\theta, \tilde{\Omega}) d\theta\, d\tilde{\Omega} \tag{7}$$

($K > 0$ normalized constant) for the Southern and Northern Hemisphere also demonstrate weaker seasonal variability in the SH (Kurgansky, 1993). Note that for the numerical calculation of informational entropy H, we used the formula (Kurganskiy and Tatarskaya, 1987)

$$H = -\sum_{\theta, \tilde{\Omega}} \tilde{\mu}(\theta, \tilde{\Omega}) \ln \tilde{\mu}(\theta, \tilde{\Omega}) / \ln N, \tag{8}$$

where $\tilde{\mu}(\theta, \tilde{\Omega})$ was normalized from the condition $\sum_{\theta, \tilde{\Omega}} \tilde{\mu}(\theta, \tilde{\Omega}) = 1$. In this case $K = (\ln N)^{-1}$, where N is the total number of cells in the discrete table for $\tilde{\mu}(\theta, \tilde{\Omega})$. Defined as (8), the informational entropy H reaches its maximal value, which is equal to 1, when the air mass is uniformly distributed over all N cells of the table. Another ultimate case of distribution is when all mass is concentrated in one cell. When $H = 0$, the value of informational entropy calculated for the real atmospheric circulation (for the mass distribution $\mu(\theta, \tilde{\Omega})$ obtained from the analysis) is between 1 and 0 and characterizes the proximity of the real atmosphere to chaos or to regular motion.

The time behavior of the PVA integral characteristics (Fig. 5) shows that the climate signal in SH is weaker than in NH, confirming the known fact that the role of nonlinear mechanisms in the formation of SH climate is more essential than in the NH climate.

3. THE EXAMPLE OF APPLYING PVA TO A GCM

The comparative calculations, based on real data and on the CPTEC (Centre for Weather Forecast and Climate Investigation) model output of some atmospheric characteristics are presented in Fig. 6-8. We have used velocity, temperature, geopotential, and surface pressure data from NCEP (National Center for Environmental Prediction) analysis and CPTEC model, for 45 days beginning on 1 September 1995. Fig. 6,a-d shows the temporal behavior of informational entropy calculated from objective analysis data and CPTEC model forecast for various regions: the entire globe, northern and southern hemispheres, area of Brazil (rectangle bounded by the latitude 0° and 25°S, and longitude 35° W and 75° W). One can see that the atmospheric motion is better organized in the NH than in the SH because the informational entropy H is smaller in the NH than in the SH. The model better reproduces the time behavior of H in

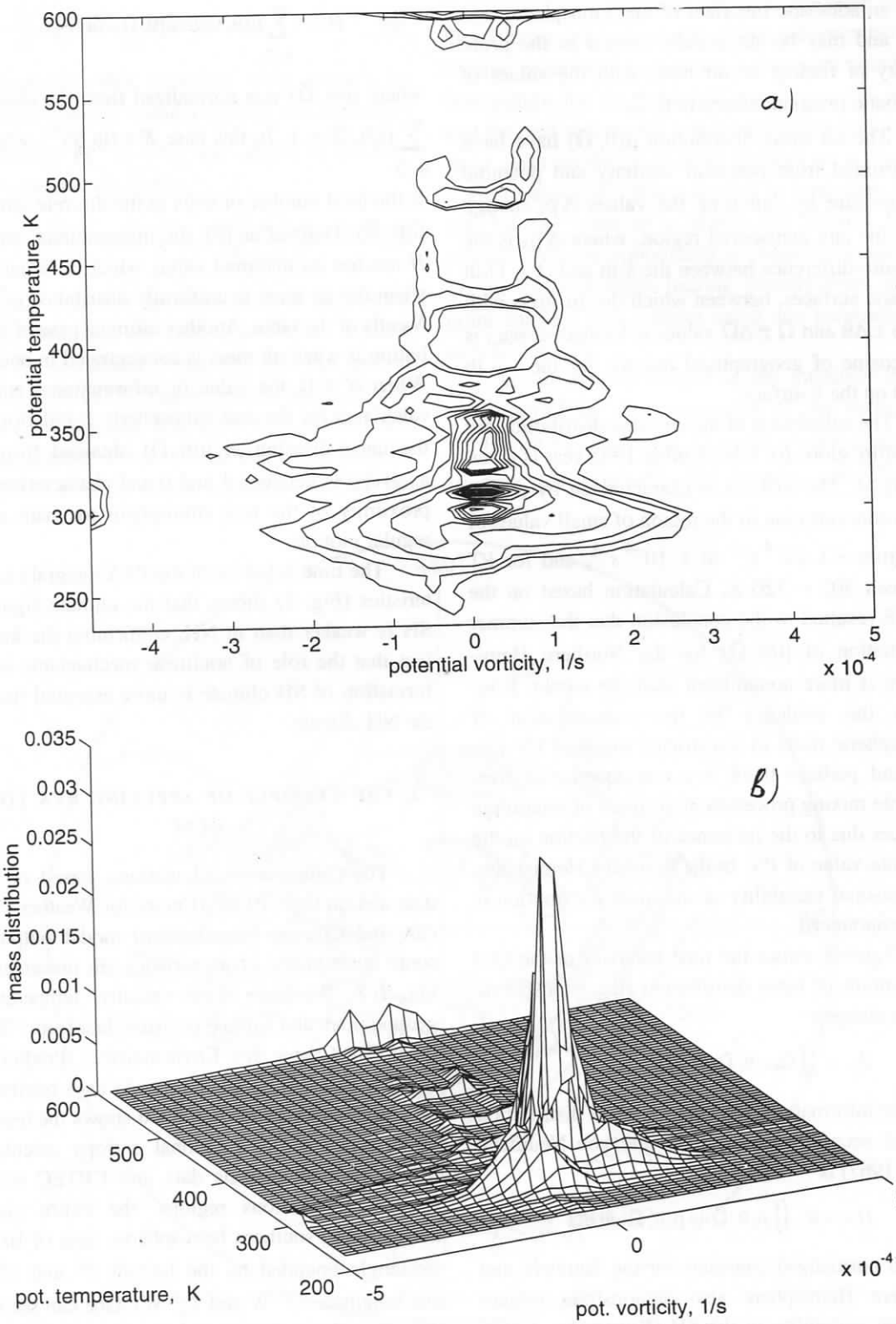

Fig. 4 — Nondimensional normalized air mass distribution in terms of potential temperature and potential vorticity for the entire Earth, 1 September 1995. a) isolines: first- 0.003, contour interval - 0.0015; b) 3-dimensional representation the same occasion.

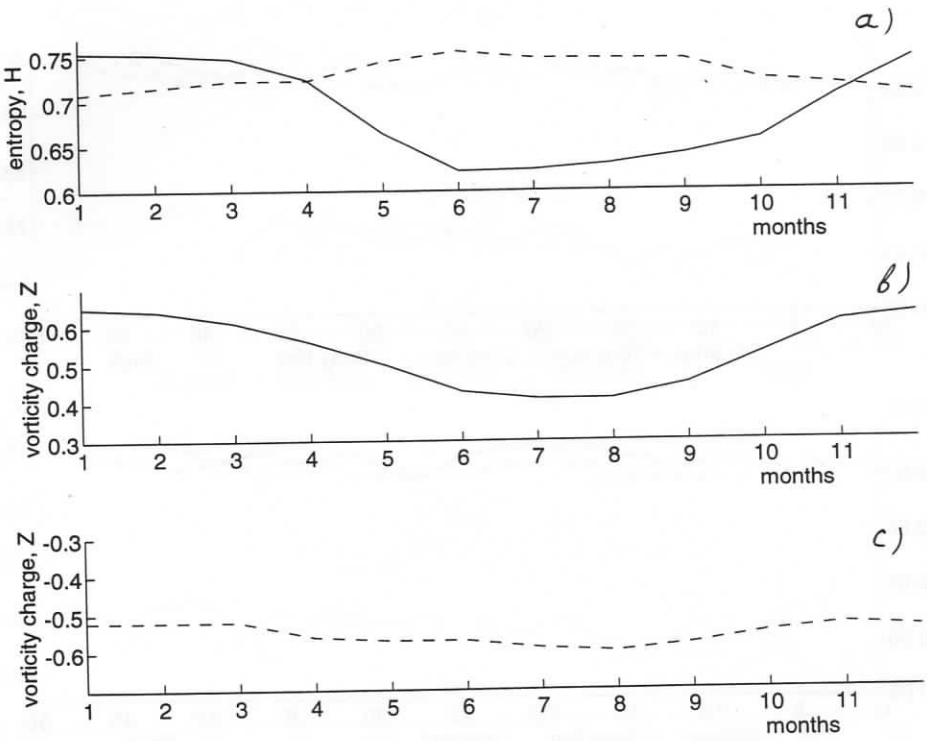

Fig. 5 — Monthly mean values (for FGGE period) of a) informational entropy for NH (___-solid line) and SH (--- - dashed line), and vorticity charge for: b) NH, c) SH.

the NH than in the SH, maybe due to the lack of data in the SH and also because the circulation in the SH is more sensitive to the drawbacks of physical parameterizations than in the NH. At the same time, for the NH it is observed a stronger decrease of informational entropy, depending on forecast day number, than in the SH. Taking into account that the atmospheric circulation in the NH has a smaller scale structure compared with the SH, this result may be a due to either a large damping for small-scale motions or that they are not very simulated.

For the entire globe, forecast and real entropies differ slightly but the correlation between forecast and analysis data is worse than for the NH and better than the SH. This is an effect of the average process. Temporal evolution of H over Brazil strongly differs from the same evolution for a other region. Only the first day forecast is approximately close to the values calculated from real data. The success of informational entropy value simulation is better viewed on Fig. 7 a-d where differences between forecast and analysis are presented. Quantitative characteristics of these curves are given in Table I. Here the correlation coefficient and the standard deviation between analysis and daily forecast are calculated on the basis of 45 days of data of the informational entropy for the above-mentioned regions. An interesting peculiarity in this table is the aggravation of the forecast quality for 3-d day in SH. We have no explanation for this fact. After analyzing the time series, we can only remark that it is not a result of bad data for some days.

Time behavior of another adiabatic functional, the vorticity charge, can be seen in Fig.8 a-d. To be more specific, Fig. 8 represent the mean potential vorticity Z_A, weighted over the atmospheric mass and it is connected to the vorticity charge of the atmosphere by the formula $Z_A = Z_A m_A$. One can make some interesting observations from Fig. 8. In the NH, the model is able to reproduce a sharp decrease of mean potential vorticity but with some time lag. The regular sharp decrease of mean po-

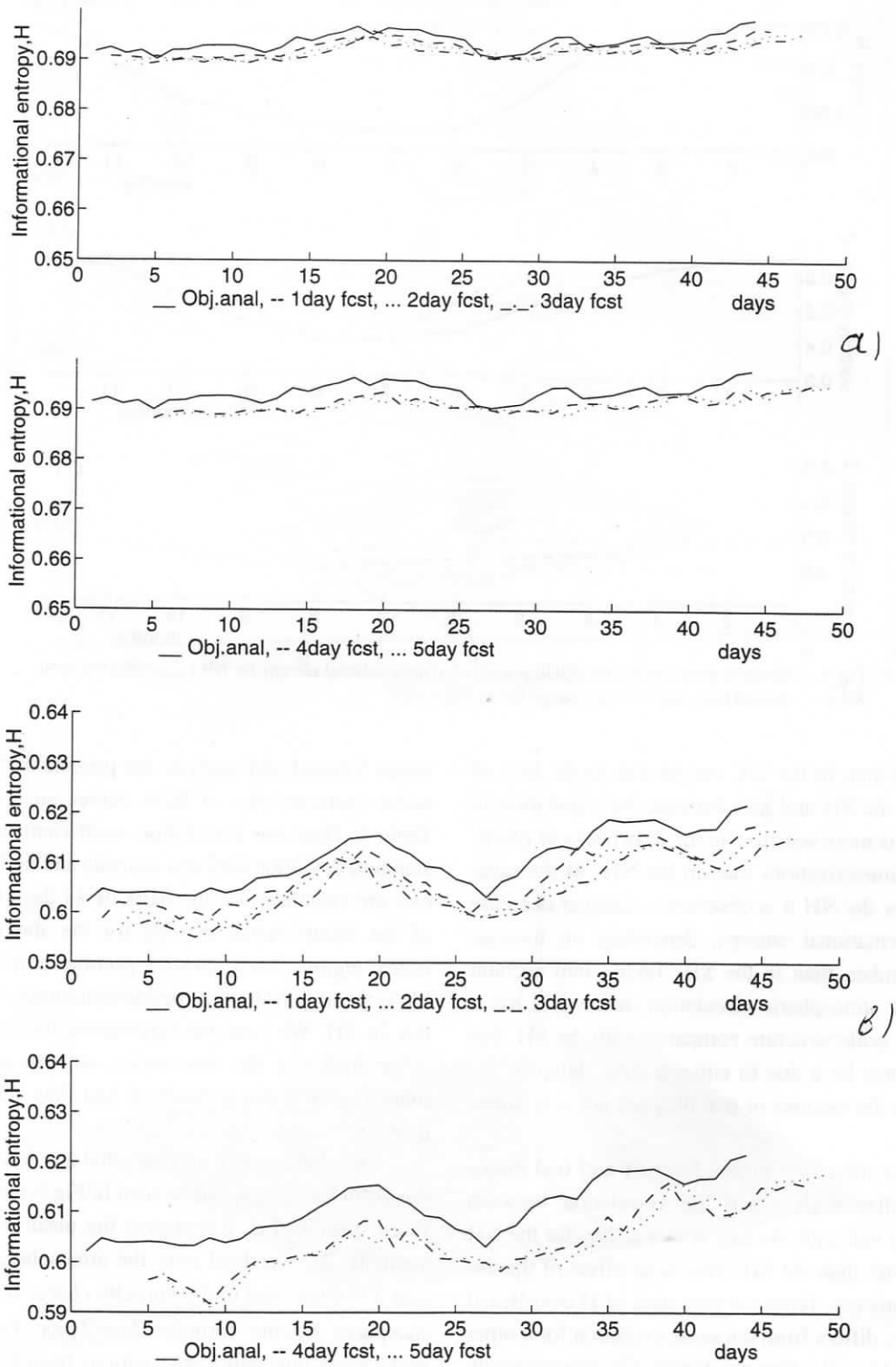

Fig. 6 — Temporal evolution of informational entropy calculated on the basis of NMC analysis data and CPTEC model data. First day is 1 September 1995. On upper graphic solid (___) line corresponds objective analysis data, (---) - 1day of forecast, (...) - 2day, (_._.) - 3day, on lower graphic solid (___) line corresponds objective analysis data, (--) - 4day of forecast, (...) - 5day. The calculations are carried out for a) entire Earth, b) NH.

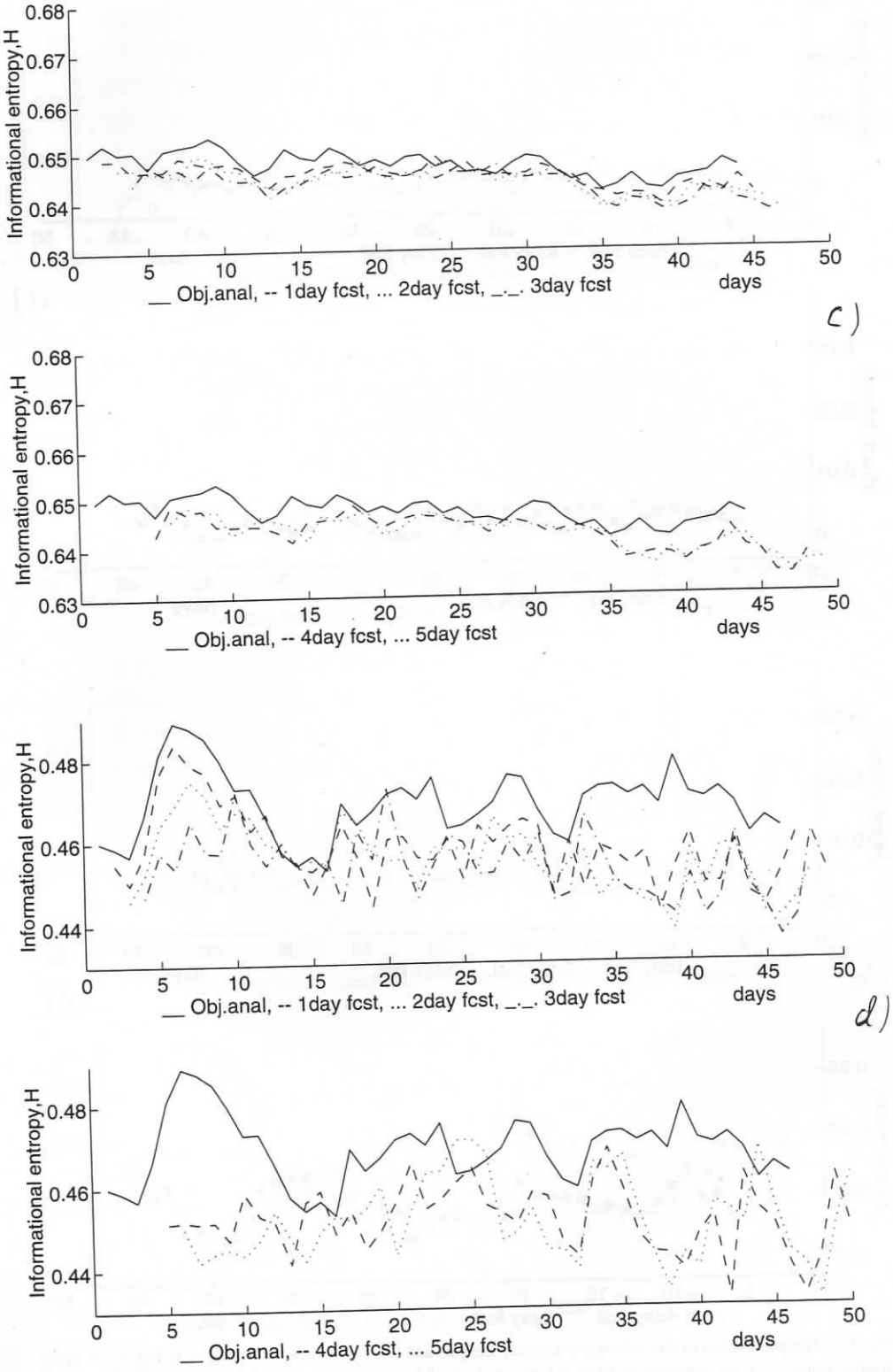

Fig. 6 — c) SH, d) area of Brazil.

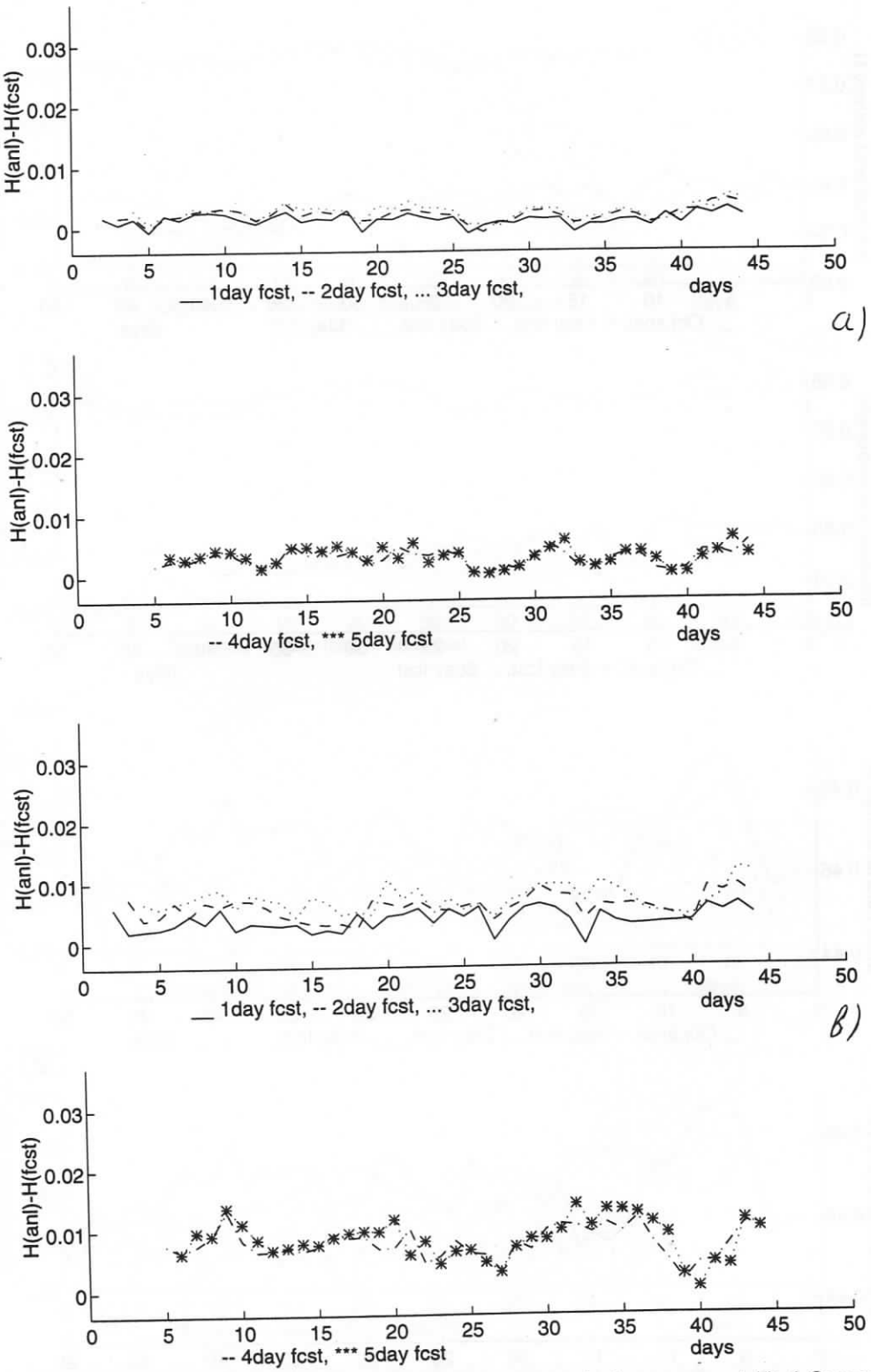

Fig. 7 — Temporal behavior the difference between analysis and forecast for the same case as in Fig. 6. On upper graphic solid (___) line corresponds 1day of forecast, (---) - 2day of forecast, (...) - 3day, on lower graphic (---) line corresponds 4day of forecast, (***) - 5day. Variant a) for the entire Earth, b) -NH.

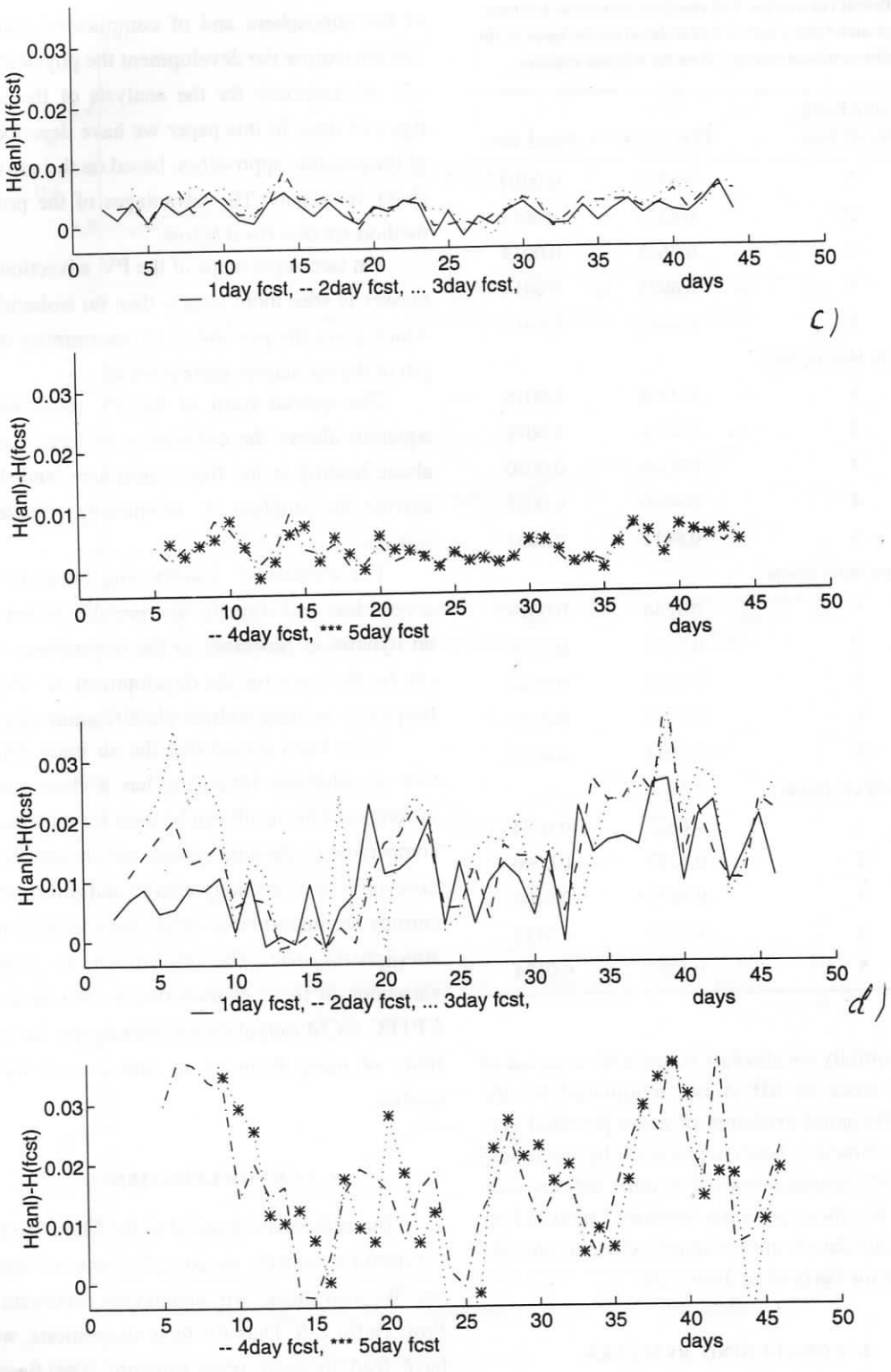

Fig. 7 — c)- SH, d)- area of Brazil.

TABLE I

Coefficient correlation and standard deviation between analysis and 5-days-forecast calculated on the basis of the informational entropy data for various regions.

Entire Earth. day of fcst.	Coef. corr.	Stand. dev.
1	0.8578	0.0010
2	0.8235	0.0011
3	0.7623	0.0013
4	0.6991	0.0014
5	0.6041	0.0015
Northern Hemisphere		
1	0.9594	0.0016
2	0.9511	0.0018
3	0.9340	0.0020
4	0.9059	0.0025
5	0.8411	0.0032
Southern Hemisphere		
1	0.7746	0.0019
2	0.7477	0.0020
3	0.6552	0.0024
4	0.7059	0.0023
5	0.7024	0.0023
Territory of Brazil		
1	0.6625	0.0074
2	0.4227	0.0090
3	0.1893	0.0104
4	0.0309	0.0111
5	-0.1293	0.0134

tential vorticity (in absolute value) with a period of about a week in SH is not reproduced by the model. Temporal evolution of mean potential vorticity for Brazil is better reproduced by the model than informational entropy. For some definite time interval, the mean potential vorticity calculated on the forecast data is approximately close to one obtained on the basis of analysis data.

4. CONCLUDING REMARKS

At present there are many approaches for investigating the general atmospheric circulation and climate. The desire to understand the behavior both of the atmosphere and of complicated numerical models require the development the physical methods of diagnostic for the analysis of the various types of data. In this paper we have described one of the possible approaches, based on the use of adiabatic invariants. The advantages of the proposed method are described below.

On isentropic maps of the PV, advection of air masses is seen more clearly than on isobaric maps which gives the possibility of determining the origin of the air masses more precisely.

The special form of the PV transformation equation allows the calculation of large-scale diabatic heating in the free atmosphere, and thus to solving the problem of monitoring climate heat sources.

The method of constructing invariant tubes gives clear and directly interpretable information on dynamical processes in the troposphere and it can be the basis for the development of the low-frequency weather regimes classification scheme.

It has been shown that the air mass distribution on adiabatic invariants has a clear seasonal difference. This result can be used for interseasonal comparison of the atmospheric circulation. Temporal evolution of vorticity charge and informational entropy are important integral characteristics of the atmospheric state. The analysis of the temporal variations of these characteristics calculated from CPTEC GCM output data demonstrates the possibility of using them as an indicator of forecast quality.

ACKNOWLEDGMENTS

The authors are grateful to Dr. Chou Sin Chan for useful comments on an earlier draft of this paper. We also thank two anonymous reviewers and Prof. Pedro L.S. Dias for their suggestions, which have lead to great improvements. The financial support of this research by CNPq is gratefully acknowledge.

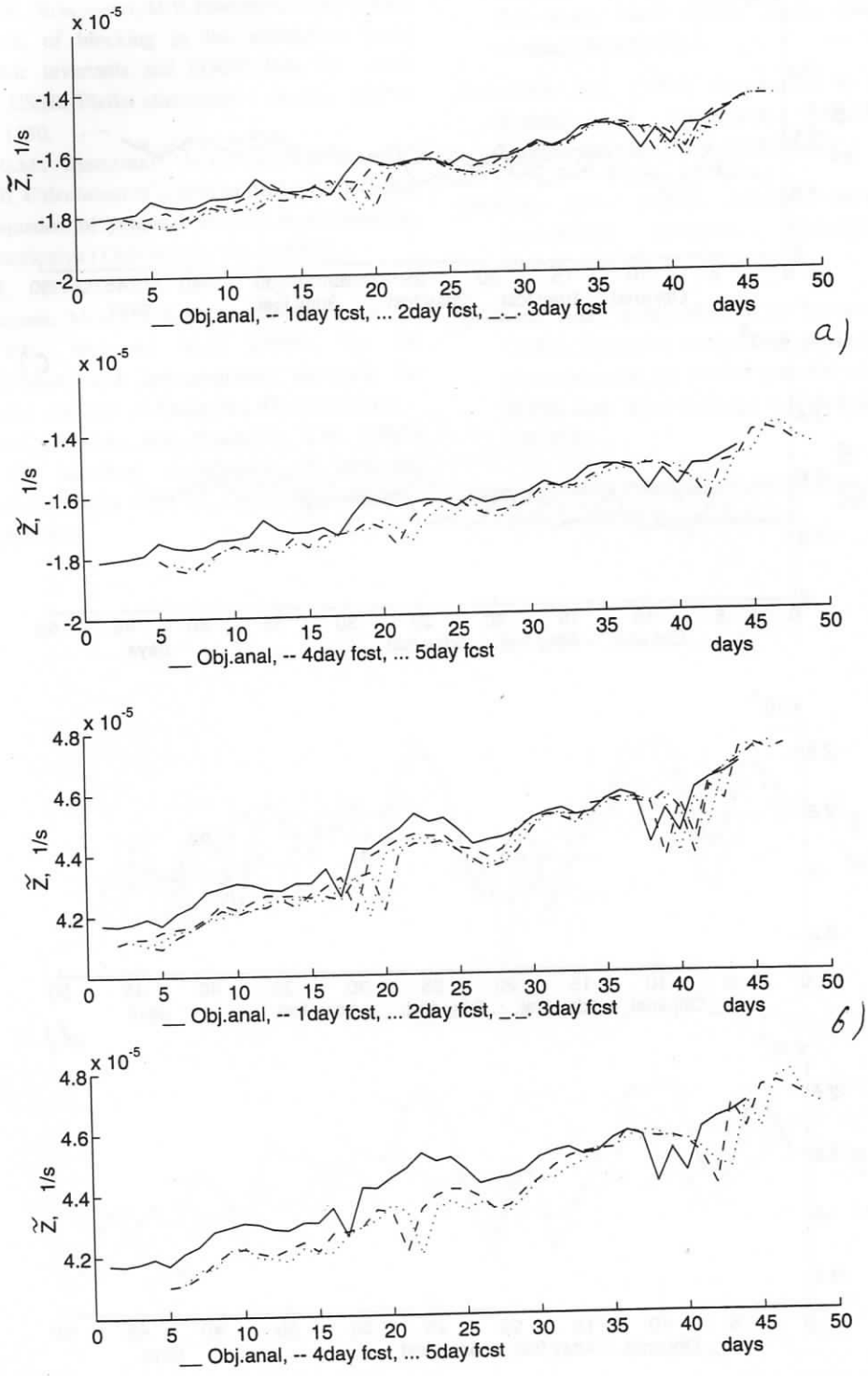

Fig. 8(A,B) — The same as the Fig.6 but for the vorticity charge.

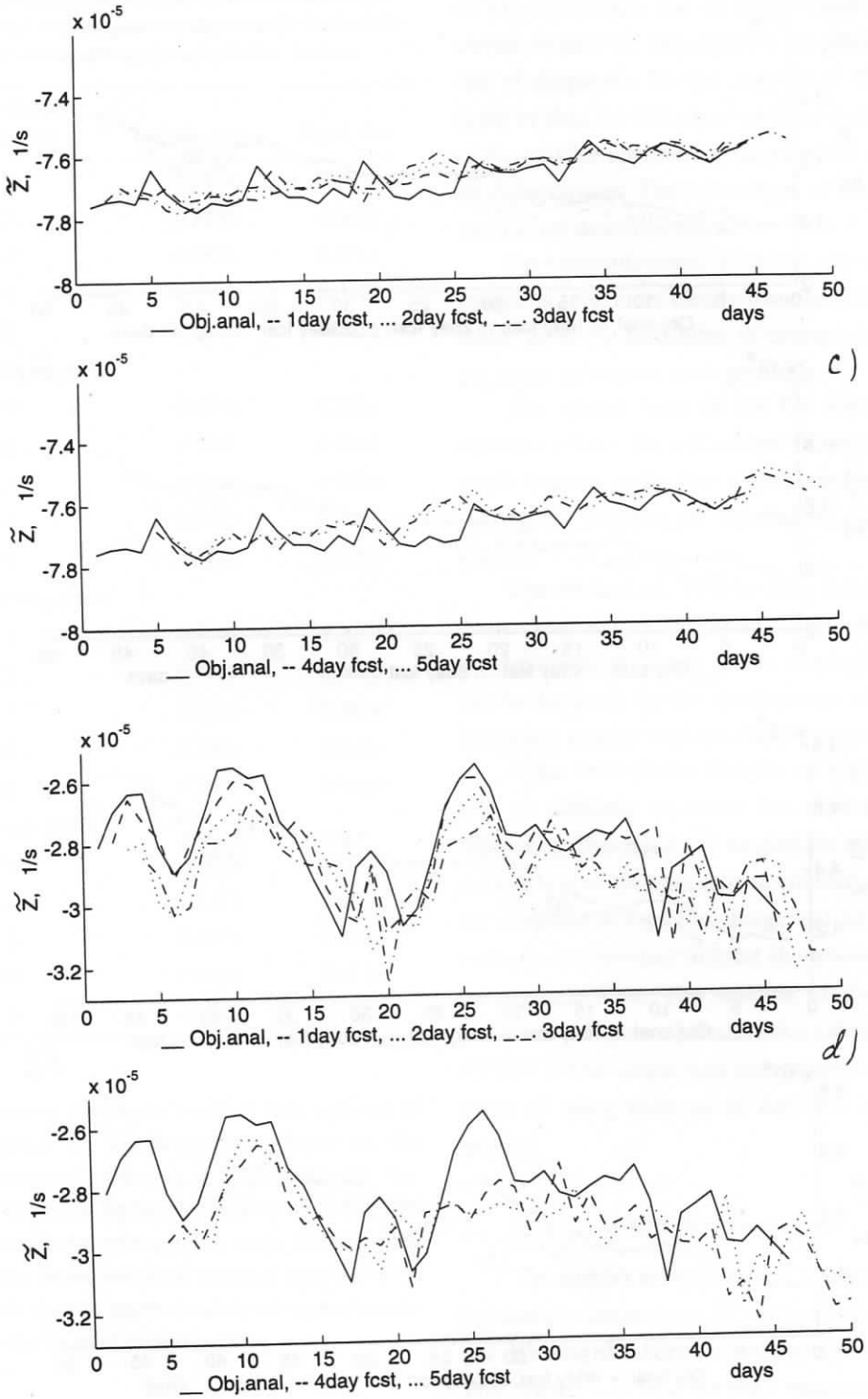

Fig. 8(C,D) — The same as the Fig.6 but for the vorticity charge.

REFERENCES

AGAYAN, G.M.; KURGANSKIY, M.V; PISNICHENKO, I.A., (1986), Analysis of blocking in the atmosphere using adiabatic invariants and FGGE data. Izv. Acad. Nauk USSR. Fizika atmospheri i okeana, **22**(11): 1123-1130.

AGAYAN, G.M.; KURGANSKIY, M.V.; PISNICHENKO, I.A., (1990), Calculation of a field of heat influxes using the equation of potential vorticity transformation. Meteorologiya i Gidrologiya, No. 7: 19-27.

ERTEL, H., (1942), Ein Neuer hydrodynamisher Wirbelsatz. Meteorol. Z, **59**(9): 277-281.

HAYNES, P.H.; MCINTYRE, M.E., (1990), On the conservation and impermeability theorems for potential vorticity. *J. Atmos. Sci*, **47:** 2021-2031.

HOSKINS, B.J.; MCINTYRE, M.E.; ROBERTSON, A.W., (1985), On the use and significance of isentropic potential-vorticity maps. *Q. J. Roy. Meteorol. Soc.*, **111:** 877-946.

KURGANSKIY, M.V.; TATARSKAYA, M.S., (1987), The use of potential vorticity in the meteorology (a review). Izv. Acad. Nauk USSR. *Fizika atmospheri i okeana*, **23**(8):787-814.

KURGANSKY, M.V., (1993), Introduction to large-scale dynamics of atmosphere, Sankt-Petersburg, Gidrometeoizdat, 168 p. (in Russian).

OBUKHOV, A.M., (1964), Adiabatic invariants of atmospheric processes. Meteorologiya i Gidrologiya, No. 2: 3-9.

OBUKHOV, A.M.; KURGANSKIY, M.V.; TATARSKAYA, M.S., (1988), Isentropic analysis of global atmospheric processes using the field of potential vorticity from FGGE data. Meteorologiya i Gidrologiya, No. 8: 111-118.

KATZ, A., (1967), Principles of statistical mechanics. San Francisco,W.N. Freeman, 240 p.